

# Magnetohydrodynamic study on the effect of the gravity stratification on flux rope ejections

Paolo Pagano<sup>1</sup>, Duncan H. Mackay<sup>1</sup>, and Stefaan Poedts<sup>2</sup>

<sup>1</sup>School of Mathematics and Statistics, University of St Andrews,  
North Haugh, KY16 9SS, St Andrews, Scotland  
email: ppagano@mcs.st-andrews.ac.uk

<sup>2</sup>Centre for mathematical Plasma-Astrophysics, K. U. Leuven ,  
Celestijnenlaan 200B, 3001, Leuven, Belgium

**Abstract.** Coronal Mass Ejections (CMEs) are one of the most violent phenomena found on the Sun. One model to explain their occurrence is the flux rope ejection model where these magnetic structures first form in the solar corona then are ejected to produce a CME. We run simulations coupling two models. The Global Non-Linear Force-Free Field (GNLFFF) evolution model to follow the quasi-static formation of a flux rope and MHD simulations for the production of a CME through the loss of equilibrium and ejection of this flux rope in presence of solar gravity and density stratification. Our realistic multi-beta simulations describe the CME following the flux rope ejection and highlight the decisive role played by the gravity stratification on the CME propagation speed.

**Keywords.** Sun, CME, Solar Corona, MHD

---

## 1. Introduction

Coronal Mass Ejections (CME's) are the main drivers of Space Weather, a term used to describe the effect of plasmas and magnetic fields on the near Earth environment.

Although not all the aspects of the CME origin have been understood, the ejection of a magnetic flux rope from the solar corona successfully describes many of the general features of CMEs, and in some of these models the flux rope naturally undergoes a loss of equilibrium Forbes & Isenberg (1991). CMEs propagate in the solar corona and interact with it. In the solar corona, plasma motions are primarily driven by the Lorentz force. However, under equilibrium conditions the plasma distribution in the corona can be described as being stratified by the effect of gravity.

Here we specifically address the role of gravitational stratification on the CME propagation. In our framework, the ejection is caused by a non-equilibrium magnetic field configuration. The non-equilibrium magnetic field is added to the stratified solar corona which is initially in equilibrium and decoupled from the magnetic field. In particular, we start from the model of Pagano *et al.* (2013) where an eruptive magnetic configuration is used and the full life span of a magnetic flux rope is described by coupling the global non linear force free model of Mackay & van Ballegoijen (2006) with MHD simulations run with the AMRVAC code Keppens *et al.* (2012). We explore how the parameter space affects the eruption characteristics by tuning both the temperature of the solar corona and the intensity of the magnetic field.

## 2. The Model

In order to study the effect of gravitational stratification on the propagation of a CME we start from the work of Pagano *et al.* (2013) where a magnetic configuration has been shown to be suitable for the ejection of a magnetic flux rope. We carry out a set of MHD simulations that consider variations in the temperature of the background coronal atmosphere and the magnetic field intensity.

We use the AMRVAC code developed at the KU Leuven to run the simulations Keppens *et al.* (2012). The code solves the ideal MHD equations and the terms that account for gravity are included and the expression for the solar gravitational acceleration is

$$\vec{g} = -\frac{GM_{\odot}}{r^2}\hat{r}, \quad (2.1)$$

where  $G$  is the Gravitational constant and  $M_{\odot}$  denotes the mass of the Sun. The configuration of the magnetic field is taken from Day 19 in the simulation of Mackay & van Ballegooijen (2006). Pagano *et al.* (2013) in Sec.2.2 explain in detail how the magnetic field distribution is imported. We assume an initial atmosphere of a constant temperature corona stratified by solar gravity, where we also allow for a small background pressure and density.

$$\rho(r) = \rho_0 e^{\frac{M_{\odot}G\mu m_p}{Tk_b r}} + \rho_{bg}, \quad (2.2)$$

$$p(r) = \frac{k_b T}{\mu m_p} \rho_0 e^{\frac{M_{\odot}G\mu m_p}{Tk_b r}} + p_{bg} \quad (2.3)$$

where we use  $\rho_0$  to tune the density at the lower boundary,  $\mu = 1.31$  is the average particle mass in the solar corona,  $m_p$  is the proton mass,  $k_b$  is Boltzmann constant and  $T$  is the temperature of the corona. We tune  $\rho_0$  depending on the temperature  $T$  in order to always have the same density at the bottom of our computational domain. Finally, we set  $\vec{v} = 0$ , as initial condition for the velocity. In the present work we use the maximum value of the magnetic field intensity of the initial magnetic field configuration,  $B_{max}$ , as a simulation parameter. The simulation domain extends over  $3 R_{\odot}$  in the radial dimension starting from  $r = R_{\odot}$ . The colatitude,  $\theta$ , spans from  $\theta = 30^{\circ}$  to  $\theta = 100^{\circ}$  and the longitude,  $\phi$ , spans over  $90^{\circ}$ . To define the MHD quantities in the portion of the domain from  $2.5 R_{\odot}$  to  $4 R_{\odot}$  we use Eq.2.2 and Eq.2.3 for density and thermal pressure and the magnetic field for  $r > 2.5 R_{\odot}$  is assumed purely radial ( $B_{\theta} = B_{\phi} = 0$ ) where the magnetic flux is assumed to be conserved. The boundary conditions are treated with a system of ghost cells. Open boundary conditions are imposed at the outer boundary, reflective boundary conditions are set at the  $\theta$  boundaries and the  $\phi$  boundaries are periodic. At the lower boundary we impose constant boundary conditions taken from the first four  $\theta$ - $\phi$  planes of cells derived from the GNLFFF model. The computational domain is composed of  $256 \times 128 \times 128$  cells distributed in a uniform grid. Full details of the grid can be found in Sec.2.3 of Pagano *et al.* (2013).

In order to analyse the role of the background stratified corona we run a set of 9 simulations using 3 different temperatures ( $T = 1.5, 2, 3 MK$ ) of the corona and 3 different maximum intensity of the magnetic field ( $B_{max} = 7, 21, 42 G$ ).

In our model, a higher corona temperature implies a more uniform density and pressure gradient and a higher amount of mass that constitutes the solar corona. At the same time, the higher temperature leads to remarkably higher  $\beta$  in the outer corona, while in the lower corona ( $r < 1.2 R_{\odot}$ )  $\beta$  is clearly below  $\sim 10^{-1}$  regardless of the temperature. The outer corona switches from a low to high  $\beta$  regime when the temperature increases from 1.5 to 3 MK.

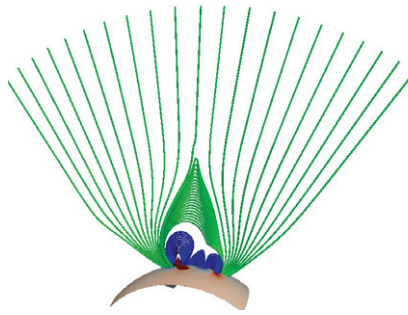


**Figure 1.** Magnetic field configuration used as the initial condition in all the MHD simulations. Red lines represent the flux rope, blue lines the arcades, green lines the external magnetic field. The lower boundary is coloured according to the polarity of the magnetic field from blue (negative) to red (positive) in arbitrary units.

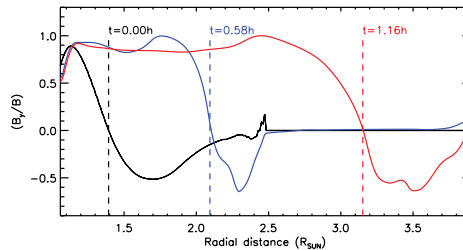


**Figure 2.** Profile of  $B_\theta/|B|$  above the centre of the LHS bipole, at different times (different colours). Dashed lines of different colours indicate where  $B_\theta/|B| = 0$ .

Simulations with different  $B_{max}$  basically differ in the plasma  $\beta$  which uniformly decreases as  $B_{max}$  increases. Thus, by changing the parameter  $B_{max}$  we globally modify the capacity of the solar corona to react to the flux rope ejection.

### 3. Results

The initial magnetic field configuration is identical in all of the simulations and it produces an ejection of the flux rope due to an initial excess of the Lorentz force. Fig.1 shows the initial magnetic configuration. The flux rope (red lines) that is about to erupt lies under the arcade system (blue lines), and external magnetic field lines (green lines) are shown above.

In the simulations, the flux rope (lying in the  $\theta$  direction) is ejected outwards and it leads to an increase in density at larger radii and the propagation and expansion of the region where the magnetic field is mostly axial, i.e.  $B_\theta/|B| \sim 1$ . This suggests that the magnetic flux rope is propagating upwards, perpendicular to its axial magnetic field lines, lifting coronal plasma.

Since the region where  $B_\theta/|B| > 0$  reproduces the CME, we use this quantity to track the ejection. Fig.2 shows the profile of  $B_\theta/|B|$  radially from the centre of the LHS bipole at different times for the simulation with  $T = 2 MK$ , and  $B_{max} = 21 G$ . The radial position where  $B_\theta/|B| = 0$  along the radial direction vertically from the centre of the LHS bipole is defined to be the top of the magnetic flux rope. In the plot in Fig.2 the top of the flux rope is at  $1.4 R_\odot$  at  $t = 0h$  (black line) and it reaches  $3.15 R_\odot$  after  $1.16h$  (red line). Some of the simulations show an ejection of the flux rope, while others show a quenched ejection. We here do not present a detailed analysis for each simulation, but plot the position of the top of the flux rope as a function of time. In Fig.3a we show the

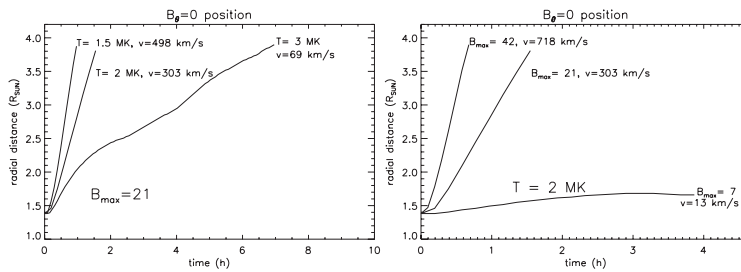


**Figure 3.** (a) Position of the top of the flux rope as a function of time in the three simulations with  $B_{max} = 21 G$ . (b) Position of the top of the flux rope as function of time in the three simulations with  $T = 2 MK$ .

position of the top of the flux rope for the simulations where  $B_{max} = 21 G$ . The speed quoted in Fig.3 is the average speed of propagation. The average speed of the CME spans a wide range from  $69 km/s$  to  $498 km/s$ . The lower is the temperature, the faster the CME. Note also that the CMEs propagating in a  $2 MK$  or  $1.5 MK$  corona are at near constant speed. Fig.3b shows the height of the top of the flux rope as a function of time for the three simulations with  $T = 2 MK$ . The higher is the magnetic field ( $B_{max}$ ) the larger the initial force due to the unbalanced Lorentz force under the magnetic flux rope and the CME travels faster. With  $B_{max} = 7 G$  we have a quenched ejection, while we have a  $718 km/s$  fast CME with  $B_{max} = 42 G$ .

#### 4. Conclusions

The present study aims at understanding the role of gravitational stratification in CMEs, and to do so we run several simulations varying the stratification temperature ( $T$ ) and plasma  $\beta$ . In all simulations an identical magnetic field configuration is used.

This study shows that gravitational stratification has an effect on the propagation of CMEs in the solar corona through the way it specifies how large the plasma  $\beta$  becomes. We also find that the plasma  $\beta$  distribution is a crucial parameter determining whether a flux rope ejection escapes the solar corona, turning into a CME, or if it just makes the flux rope find a new equilibrium at a higher height. Similarly we find that a cooler solar corona ( $T \sim 1.5 MK$ ) can help the escape of the CME and make it travel faster. The gravitational stratification turns to play a role because the coronal stratified plasma reacts to the perturbation due to the flux rope ejection with thermal pressure gradients contrasting the motion. However, these gradients have a significant effect (either in quenching the ejection or braking it), only when we depart from the low  $\beta$  regime in which the Lorentz force completely governs the dynamics.

However, the domain of application of the current work is limited to the coronal events where we find similar values of plasma parameters and magnetic field intensity. Therefore, it can be certainly applied to large quiescent and intermediate prominences that have moderate magnetic fields, but in active region filaments the magnetic field is significantly more intense and thus the plasma  $\beta$  significantly low in spite of the coronal temperature. In such circumstances, the gravitational stratification is likely to play no role.

#### References

- Pagano, P. and Mackay, D. H., & Poedts, S. 2013, *A&A*, 554, A77  
 Forbes, T. G. & Isenberg, P. A. 1991, *ApJ*, 373, 294  
 Mackay, D. H. & van Ballegoijen, A. A. 2006, *ApJ*, 641, 577–589  
 Keppens, R., Meliani, Z., van Marle, A. J., Delmont, P., Vlasov, A., & van der Holst, B. 2012, *Journal of Computational Physics*, 231, 718–744